Arabian Journal of Geosciences (2020) 13: 898
https://doi.org/10.1007/s12517-020-05879-6

2ND CAJG 2019

The use of sodium chloride as strategy for improving CO_2/CH_4 replacement in natural gas hydrates promoted with depressurization methods

Alberto Maria Gambelli[1] · Federico Rossi[1]

Received: 11 March 2020 / Accepted: 20 August 2020 / Published online: 3 September 2020

Abstract

Natural gas hydrates represent a valid opportunity in terms of energy supplying, carbon dioxide permanent storage and climate change contrast. Research is more and more involved in performing CO_2 replacement competitive strategies. In this context, the inhibitor effect of sodium chloride on hydrate formation and stability needs to be investigated in depth. The present work analyses how NaCl intervenes on CO_2 hydrate formation, comparing results with the same typology of tests carried out with methane, in order to highlight the influence that salt produced on hydrate equilibrium conditions and possibilities which arise from here for improving the replacement process efficiency. Sodium chloride influence was then tested on five CO_2/CH_4 replacement tests, carried out via depressurization. In relation with the same typology of tests, realised in pure demineralised water and available elsewhere in literature, three main differences were found. Before the replacement phase, CH_4 hydrate formation was particularly contained; moles of methane involved were in the range 0.059–0.103 mol. On the contrary, carbon dioxide moles entrapped into water cages were 0.085–0.206 mol or a significantly higher quantity. That may be justified by the greater presence of space and free water due to the lower CH_4 hydrate formation, which led to a more massive new hydrate structure formation. Moreover, only a small part of methane moles remained entrapped into hydrates after the replacement phase (in the range of 0.023–0.042 mol), proving that, in presence of sodium chloride, CO_2/CH_4 exchange interested the greater part of hydrates. Thus, the possibility to conclude that sodium chloride presence during the CO_2 replacement process provided positive and encouraging results in terms of methane recovery, carbon dioxide permanent storage and, consequently, replacement process efficiency.

Keywords Natural gas hydrates · Chemical inhibitors · Sodium chloride · CO_2/CH_4 exchange · Replacement process efficiency

Introduction

Gas hydrates are ice-like crystalline solid compounds, where, in presence of suitable conditions of relatively low temperature and high pressure, small gaseous molecules, also called "guests", are trapped inside a hydrogen bonded network of water molecules, called "hosts" (Sloan and Koh 2008; Sloan Jr. 2003). The most important difference, existing between water cage structures typical of hydrates and normal ice, is the formation of polyhedral structures, which hydrates guarantee enough space for containing non-polar guest molecules (Moridis et al. 2009). Hydrate structures may involve lots of different "host" molecules; among them, the most investigated and researched are hydrocarbons, i.e. methane (CH_4), ethane (C_2H_6) and propane (C_3H_8) (Sloan Jr. 2003). However, solutions of interest consist in hydrates composed by carbon dioxide, flue–gas mixtures, ammonia and so on (Shin et al. 2012). Natural gas hydrates (NGH) are diffused in deep oceans and in permafrost regions, or elsewhere, thermodynamic conditions are suitable and natural gas is present in presence of water (Mori 2003).

Both the scientific and industrial interests on gas hydrate were born from their several possible applications, in terms of gas storage, energy production, carbon dioxide sequestration, gas separation and desalination (Sun et al. 2018a, 2018b). Moreover, it is completely justified by quantities: the energy

This paper was selected from the 2nd Conference of the Arabian Journal of Geosciences (CAJG), Tunisia 2019

Responsible Editor: Santanu Banerjee

✉ Alberto Maria Gambelli
alberto.mariagambelli@gmail.com

[1] University of Perugia, Engineering Department, Via G. Duranti 67, 06125 Perugia, PG, Italy

producible from hydrocarbons contained into hydrates is at least two times higher than energy which can be produced from all conventional energy sources put together (Gambelli 2018). Also considering that, in presence of standard conditions of temperature and pressure, 1 m^3 of NGH corresponds to 164 m^3 of released methane (Boswell and Collett 2011), hydrates are nowadays considered one of the most promising high-density energy sources.

Several strategies for realizing the CO_2 replacement have been performed; from these, the most known are depressurization, thermal stimulation, chemical inhibitor injection and a combination of them (Gambelli 2018). Depressurization strategies are based on reducing hydrate reservoir pressure without varying temperature, in order to move thermodynamic conditions far from the equilibrium area, or the hydrate stability zone (HSZ) (Li et al. 2015; Myshakin et al. 2016). With thermal stimulation, the opposite strategy than depressurization is performed: reservoir pressure remains unchanged, while temperature is increased for going out from the HSZ (Lee et al. 2018; Gambelli and Rossi 2019). The use of chemical inhibitors, such as alcohols or sodium chloride, allows to move—in correspondence of their injection—hydrate equilibrium conditions to lower temperature and higher pressure values; thus, because P–T conditions of the reservoir remain the same, water cage dissociation is provided (Liang et al. 2018). The inhibitor effect of inorganic salts is related to their capability of reducing water activity in the surrounding liquid phase, hindering hydrates formation due to the lack of free water molecules (Xu and Li 2014). Nowadays, the scientific research is particularly involved in performing the CO_2 replacement process (Sun et al. 2018c). That method consists in injecting carbon dioxide inside NGH reservoirs, in order to get methane and, at the same time, store CO_2 (Babu et al. 2015). The permanent storage of carbon dioxide into water cages previously occupied by methane molecules allows to two important consequences: firstly, NGH reservoirs might become a carbon neutral energy source (even if it is true only evaluating an ideal efficiency of the replacement process, where all methane molecules recovered will be replaced with an equal number of carbon dioxide molecules); moreover, the insertion of another gas compound for replacing methane permits to avoid water cage dissociation (Linga et al. 2007). Where present, hydrate structures play a key role in terms of seafloor stability (Ginsburg and Soloviev 1998; Paull and Dillon 2001). Several researches were carried out for defining the relation existing between mechanical properties of hydrate-bearing sediments and seafloor deformation (Mel'nikov and Kalashnik 2011). Sultan et al. (2004a, 2004b) attributed the responsibility of soil resistance reduction to the excess of pressure in rock pores caused by hydrate dissociation. The applicability of CO_2/CH_4 exchange into water cages is based on the differences in thermodynamic equilibrium conditions which hydrates assume in function of the "host" gaseous specie: carbon dioxide is capable to constitute hydrates at lower pressure and/or higher temperature values than methane hydrates. That difference generates a thermodynamic region between CO_2 and CH_4 equilibrium curves, which can be exploited for promoting the replacement process.

Fig. 1 Image of the reactor used for hydrate formation and CO_2/CH_4 replacement into water cages

A more effective solution for NGH reservoir exploitation consists in coupling different strategies: in this sense, the most applied and verified combination forecasts the simultaneous use of depressurization and thermal stimulation (Gambelli et al. 2019a). In this work, we investigated the effect produced by sodium chloride presence on carbon dioxide hydrate formation, in order to propose a new further possibility: the combination of CO_2/CH_4 replacement process with the use of chemical inhibitors. If the hindering effect of NaCl presence for hydrates is well known and widely documented in literature (Yu et al. 2018), the possibility that it could make the CO_2 replacement process more feasible or not needs to be deepened. Previous works (Gambelli et al. 2019b) proved how the application of a CO_2 replacement method on methane hydrate core may be favoured, in terms of efficiency, in presence of sodium chloride. In tests performed in these works, the percentage of carbon dioxide present into water cages was higher than in case of absence of salt (or using pure demineralised water).

In the first part of the present work, the CO_2 hydrate formation process was tested both in demineralised water and in a aqueous solution containing 37 g/l of NaCl. That specific value was selected by taking into account that the greatest number of marine NGH reservoirs are situated in regions where water salinity is in the range 30–37 g/l. In the second part, some whole replacement tests were carried out; the method adopted, for promoting methane escaping and carbon

Table 1 Reactor's internal volume specifications

Board height	21	cm	Internal pipe volume	1	cm^3
Internal height	22.1	cm	Volume of intake pipes	18	cm^3
Depth from the edge	18.5	cm	Gas volume from the high edge	90	cm^3
Depth edge to the network	18.3	cm	Total volume of free gas	109	cm^3
Weld thickness	1.1	cm	Internal reactor volume	949	cm^3
Thickness from the edge	1	cm	Total reactor volume	950	cm^3
Internal diameter	7.4	cm			

dioxide entrapping, was depressurization. For each test, the quantity of formed CH_4 hydrates before the replacement phase, the amount of CO_2 involved in the process and the difference between hydrate moles present immediately before and after the replacement process were analysed.

Experimental apparatus

The experimental apparatus was designed for reproducing a sea bed natural gas hydrate deposit and then recovery methane (Rossi et al. 2019; Gambelli et al. 2019c), contained into water cages, via CO_2 replacement strategies. It has already been used in previous works; thus, a more deepened description of its characteristics and performance (several scientific reports highlight a relation between reactor's geometrical characteristics and hydrate formation efficiency (Gambelli et al. 2019a; Shagapov et al. 2017)) may be found elsewhere in literature. The whole reactor is made with 316SS stainless steel; its internal volume is about 949 cm^3 and describes a cylinder, with 7.3 cm diameter and 22.1 cm height. The lateral surface has a wall thickness of 0.76 cm, while the upper and lower section are sealed with two flanges, having 4.7 cm thickness. The reactor is visible in Fig. 1.

The structure is capable to reach a pressure equal to 150 bar; over that value, a safety valve guarantees the gas outgoing from the reactor for avoiding danger situations for operators and reactor breakages. Methane is injected from the lower flange, while carbon dioxide from the upper. That configuration permits a good approximation of interventions in real NGH deposit, where CH_4 contained into hydrates usually comes from the floor, while CO_2 is introduced from the upper area. Between gas cylinders and the reactor, two flowmeters (model El–Flow F–112AC, by Bronkhorst) were inserted for measuring quantities injected inside. A further channel for gas flowing is present in the upper flange: it performs the dual function of gas ejection, when it is necessary, and, thank to a porous septum, provides the possibility of taking samples for gas analysis. For internal volume considerations, also pipe volume before closure due to valve presence was considered. More detailed information is provided in Table 1.

Two further channels are present in the upper flange for the insertion of, respectively, a digital manometer and four thermocouples inside the reactor. The manometer, model MAN–SD by Kobold, has an accuracy equal to ± 0.5% of full scale. About temperature, four type K thermocouples were selected, with class accuracy 1. They were disposed at four different depths, in order to better control the process evolution during experiments. Starting from the top surface, thermocouples are

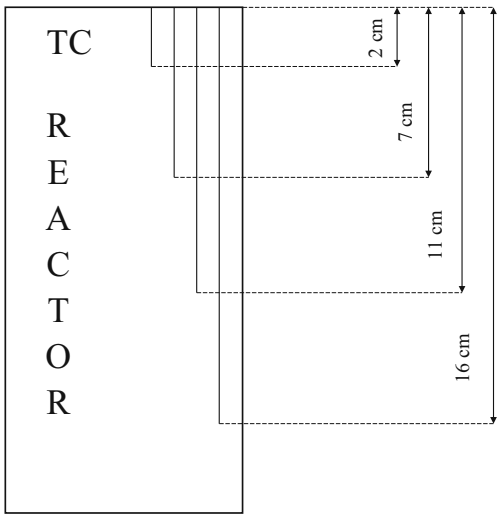

Fig. 2 Thermocouples positioning inside the reactor and relative depths

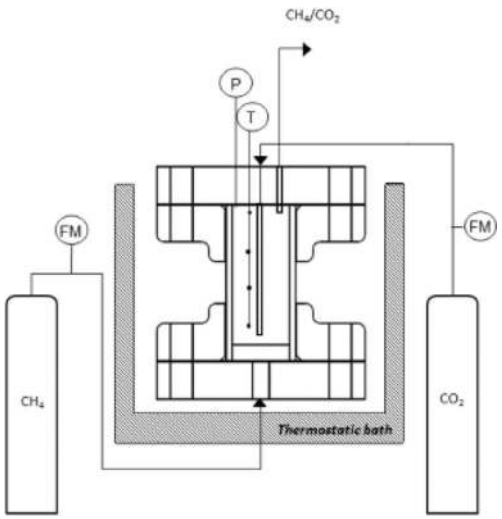

Fig. 3 Scheme of the completely assembled experimental apparatus

Table 2 Pressure, temperature and moles values related to tests realised in absence of salt

	P_i [bar]	T_i [°C]	Z_i	P_f [bar]	T_f [°C]	Z_f	CO_{2hyd} [mol]
Test 1	27.43	7.33	0.86	17.48	1.57	0.89	0.102
Test 2	25.23	6.51	0.84	17.09	2.86	0.89	0.083

positioned, respectively, at 2, 7, 11 and 16 cm depths. Their positioning is also described in Fig. 2.

While pressure is controlled by injecting different gas quantities inside the reactor, for temperature condition regulation, the reactor was inserted in a thermostatic bath, filled with a mixture of water and glycol. Temperature is regulated with a chiller (model GC–LT by Euro–chiller), which controls glycol flow into a double cupper coil, which is positioned in the internal part of the vessel lateral surface and modifies bath temperature, thus, indirectly, the reactor one. Finally, a scheme of the completely assembled experimental apparatus is shown in Fig. 3.

Materials

For better simulating a real seafloor NGH reservoir, the reactor was filled with sand (0.744 l) and distilled water (0.236 l). Sand consists in quartz spheres having 500 μ and porosity equal to 34%. Porosity was measured with a porosimeter, model Thermo Scientific Pascal 140. In tests carried out with sodium chloride, that compound was obviously added, with a concentration of 37 g/l. Methane and carbon dioxide used for hydrate formation have a certification of ultra-high purity degree (UHP), with purity, respectively, equal to 99.97% and 99.99%.

Methods

The first part of experiments carried out describes carbon dioxide hydrate formation in presence and in absence of salt. In both cases, tests were carried out with the same procedure. Firstly, temperature was reduced until reaching values suitable for hydrate formation; the temperature range selected was 2–4 °C. Then, CO_2 injection started; consequently, pressure increased until reaching the desired value. As soon as

Table 3 Pressure, temperature and mole values related to tests realised in presence of salt

	P_i [bar]	T_i [°C]	Z_i	P_f [bar]	T_f [°C]	Z_f	CO_{2hyd} [mol]
Test 3	32.01	6.66	0.80	26.34	1.68	0.83	0.068
Test 4	29.93	6.59	0.81	24.26	3.60	0.85	0.058

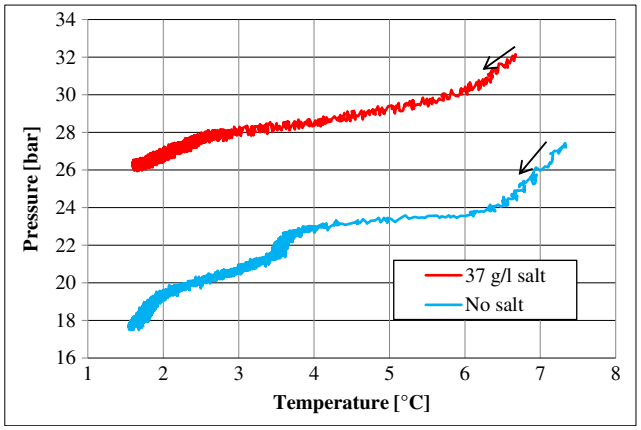

Fig. 4 Pressure vs temperature: comparison between test 1 (in blue) and test 3 (in red)

thermodynamic conditions made the process feasible, hydrate formation begun. The process is exothermic, so hydrate formation is accompanied by a sudden temperature increase. In correspondence of it, pressure started decreasing, due to gas molecule entrapment into solid crystalline water cages. Pressure continued decreasing until reaching the equilibrium value (which is related to the local temperature). Moles of carbon dioxide involved in hydrate formation were calculated using the following equation:

$$n_{hyd} = \left[V_{pore}(P_i{*}Z_f\text{-}P_f{*}Z_i)\right] / \left[Z_f{*}\left(RT\text{-}P_f/\rho_{hyd}\right)\right] \quad (1)$$

where n_{hyd} are the CO_2 moles entrapped into hydrate, Z is the compressibility factor, calculated using the Peng–Robinson equation, V_{pore} represents the sand pore volume and ρ_{hyd} is the hydrate ideal molar density and was calculated by using a density value from literature equal to 91 g/cm^3 (Aregba 2017; Takeyaa et al. 2006).

The second part of experiments did not describe only hydrate formation but concerned also CO_2/CH_4 replacement. Firstly, methane hydrates were formed in the same way previously described for CO_2 hydrates; then, CO_2/CH_4

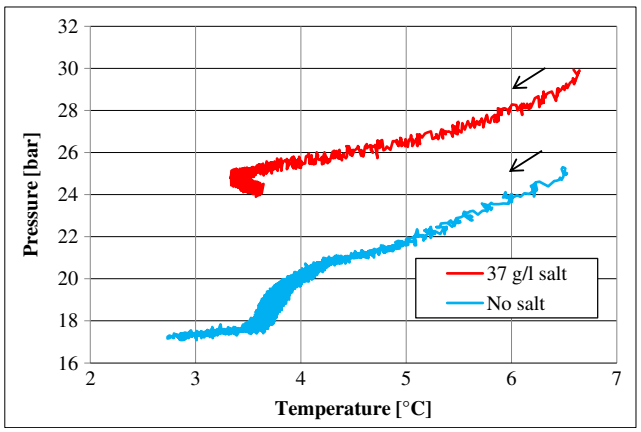

Fig. 5 Pressure vs temperature: comparison between test 2 (in blue) and test 4 (in red)

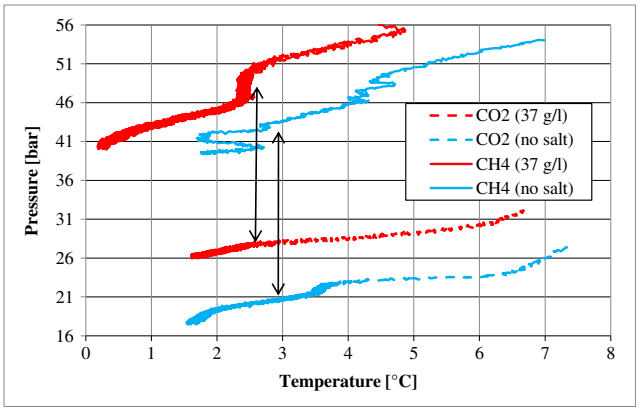

Fig. 6 Comparison between four different hydrate equilibrium curves: CO_2 is represented with the blue colour, while CH_4 with the red one; tests realised without salt are dashed, while the continuous line describes tests carried out in presence of 37 g/l of sodium chloride

replacement was performed via depressurization: once CH_4 hydrate formation finished, the reactor was put in communication with the external for both injecting inside CO_2 and eject CH_4. In this way, a mixture of both species was ejected, while only pure carbon dioxide entered. After that, the reactor was closed and the replacement phase occurred. Once the process finished, respective quantities of CO_2 and CH_4 involved into hydrates were evaluated by making gas–chromatographic analysis. Two different devices were used for analysis: Molsieve 5A to detect methane and Poraplot PPU for carbon dioxide. In all cases, measured uncertainty stays in the third decimal place of output values.

Results and discussion

The first part of this section shows two hydrate formation tests, realised in presence of salt water (37 g/l of sodium chloride) and, then, compared with two other tests performed in pure demineralised water. The most relevant parameters about tests carried out without salt are shown in Table 2, while the same information for tests realised in presence of salt is in Table 3.

In these tables, P and T represent, respectively, pressure and temperature, while subscripts "I" and "f" describe the moment in which the hydrate formation process began and when it finished. Compressibility factor is indicated with letter Z and was calculated with the Peng–Robinson equation. Finally, parameter CO_{2hyd} shows the quantity (in moles) of carbon dioxide involved into hydrates. The capability of carbon dioxide to dissolve in water cannot be neglected; for this reason, the quantity of carbon dioxide involved into hydrates was calculated considering both the total amount of gas injected inside the reactor and the quantity dissolved in water, which was evaluated using the Henry law. In particular, this last value can be included in the hydrate counter; in fact, the presence of suitable thermodynamic conditions makes sure that, with the past of the time, dissolved CO_2 will be entrapped into water cages. The following figures show a comparison between tests carried out in absence and in presence of salt. Figure 4 makes a comparison between test 1 and test 3, while Fig. 5 is referred to test 2 and test 4.

In both diagrams, the black arrows indicate the time direction. Hydrate formation describes a pressure reduction, due to the entrapment of gas molecules into solid structures. Also, temperature decreased: the initial formation led to a sudden increase from the thermostatic bath value to peaks shown in the tables among, while temperature decrease visible in these diagrams shows the restoration of thermal equilibrium, which is constantly and slightly hindered by heat produced with the progress of hydrate formation. Salt presence clearly affects hydrate equilibrium: for similar temperature values, pressure is significantly higher in tests carried out in presence of salt. In previous works (Gambelli et al. 2019b), the same comparison was made for methane hydrates, reaching the same final conclusions, or the inhibitor effect which sodium chloride

Table 4 Parameters describing methane hydrate formation phase for all replacement tests

Methane hydrate formation					
	Test A	Test B	Test C	Test D	Test E
V [cm^3]	235	235	235	235	235
P_i [bar]	60.27	60.28	60.71	61.75	58.27
T_i [°C]	3.90	− 0.03	2.63	3.59	2.54
Z_i	0.82	0.81	0.82	0.82	0.82
P_f [bar]	55.25	56.34	54.99	56.44	50.79
T_f [°C]	0.12	0.73	2.73	0.82	0.03
Z_f	0.83	0.83	0.83	0.82	0.84
nCH_{4inj} [mol]	0.750	0.770	0.759	0.769	0.729
nCH_{4hyd} [mol]	0.061	0.070	0.080	0.059	0.103

Table 5 Parameters describing CO_2/CH_4 exchange phase for all replacement tests

CO_2/CH_4 replacement phase					
	Test A	Test B	Test C	Test D	Test E
P_i [bar]	35.26	35.13	26.71	38.74	29.60
P_f [bar]	36.11	34.72	30.83	38.94	32.23
P_{diss} [bar]	12.15	12.87	14.87	24.56	11.68
T_{diss} [°C]	-0.03	0.30	3.24	7.42	0.16
n_{diss} [bar]	0.126	0.133	0.152	0.247	0.121
CH_{4diss} [%]	18.21	21.07	27.66	16.89	29.98
CO_{2diss} [%]	81.79	78.93	72.34	83.11	70.02
nCO_{2hyd} [mol]	0.103	0.105	0.110	0.206	0.085
nCH_{4hyd} [mol]	0.023	0.028	0.042	0.042	0.036

provides on hydrate formation. Topic of the present paper is to give a contribution in the determination of a possible selective behaviour of salt in function of the "guest" specie involved into hydrates. The inhibitor effect of NaCl on the process is widely proved in literature; however, not enough information exists about its possible selective behaviour. The topic of this work is graphically shown in Fig. 6, where equilibrium diagrams of CO_2 and CH_4 formation tests, carried out both in presence and in absence of salt, were compared.

Methane tests here proposed were previously shown in Gambelli et al. (2019b) and were selected properly for well comparing how proved here with carbon dioxide with consideration made in that work, making the same experiments, but with methane.

The present comparison allows to make some further considerations. First of all, the experimental equilibrium curve better approximates the theoretical one for lower pressure values. It depends by different factors. Considering the reactor dimensions (typical of a lab-scale apparatus), a greater pressure value may trigger the hydrate formation reaction in different areas of the experimental environment and in different time periods. That phenomenon is observed in P–T diagrams with a temporary deviation from the trend and can also be observed in Fig. 6: the left side of CO_2 curve realised in presence of salt clearly describes that. Moreover, it was observed in several scientific works: Shagapov et al. (2017) explained how kinetic has a key role in experiments carried out in small size reactors. In particular, pressure is directly linked to sand pore saturation degree and the experimental process is nearer to the theoretical one for lower sand saturation values. The thermodynamic region available for CO_2/CH_4 exchange consists in the strip existing between CH_4 and CO_2 equilibrium curves in P–T diagrams. In function of pressure, temperature, gas concentration, partial pressure of each "guest" specie involved, sand porosity and others, these two diagrams may show some different behaviours. This work suggests that also water salinity might be considered part of the previous list of factors. While NaCl inhibitor effect is well known, the possibility that its effect may be stronger or weaker depending on pressure, temperature, porosity and, mostly, in function of the "guest" specie needs to be deepened. Experiments shown in Fig. 6 suggest that, during hydrate formation, CH_4 and CO_2 diagrams, due to sodium chloride presence, may vary in different ways from each other. If that variation leads to curve removal, the greater space between them will guarantee a higher CO_2 replacement process efficiency.

That thesis was now supported with data obtained from five complete CO_2 replacement tests, carried out in presence of salt. As explained previously, depressurization was adopted as strategy for performing CO_2/CH_4 replacement. Table 4 summarises all parameters of interest about hydrate formation phase of these tests, while Table 5 shows the CO_2/CH_4 replacement process. The following figures describe pressure and temperature trend over time for all of them.

Letters and subscript here present and also used previously in the text have the same meaning specified before. Reactor internal free volume is shown with letter "V" and is the difference between the overall volume (949 cm^3) and portions occupied by quartz sand (491 cm^3) and water (236 cm^3). Sand volume portion needs to be better specified: it occupies 744 cm^3 but the presence of internal pores, which characterise the

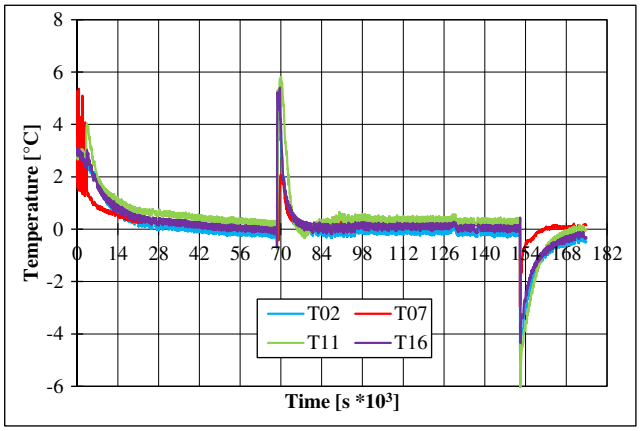

Fig. 8 Temperature over time in test A

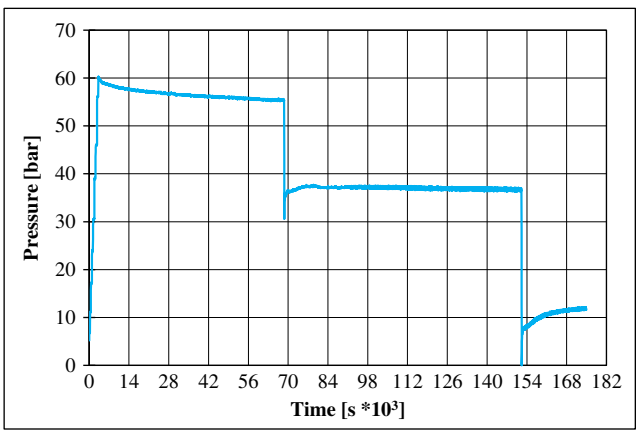

Fig. 7 Pressure over time in test A

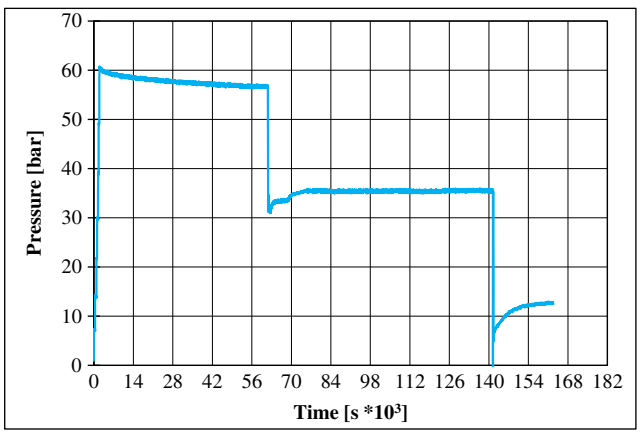

Fig. 9 Pressure over time in test B

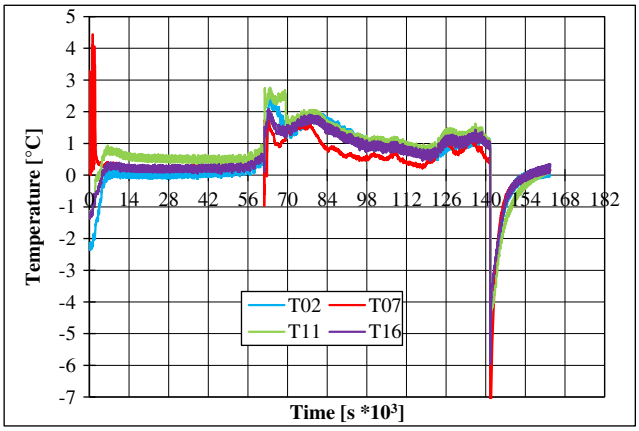

Fig. 10 Temperature over time in test B

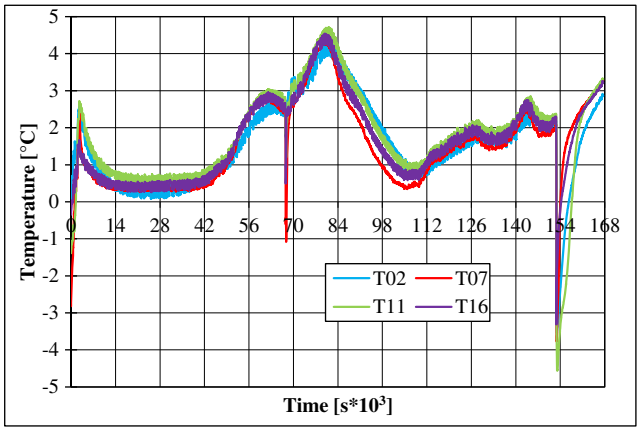

Fig. 12 Temperature over time in test C

total volume for 34%, has to be taken into account. Considering volumes described by channels used for gas injection or measure device insertion, the total free volume available for gas injection is properly 235 cm^3. In Table 4, parameters nCH_{4inj} and nCH_{4hyd} describe, respectively, moles of methane injected inside the reactor and the respective part involved in hydrate formation. In Table 5, P_i and P_f have the same meaning of their respective in Table 4, but are referred to the replacement process. P_{diss} and T_{diss} are indicated pressure and temperature reached inside the reactor once hydrate dissociation was completed. In this case, temperature was used for evaluating moles of gas entrapped into hydrates (n_{diss}), whose composition was established via gas-chromatographic analysis (CH_{4diss} and CO_{2diss}). Finally, considering moles of formed hydrates and percentages of both species, the mole quantity of carbon dioxide and methane entrapped into water cages was calculated (nCO_{2hyd} and nCH_{4hyd}).

Seen in Table 4, moles of CH_4 formed in the first phase in significantly lower than the same value related to tests carried out in absence of salt. According to how present in literature, the introduction of sodium chloride, while keeping the same test setting, led a decrease in moles of hydrates formed. However, moles of carbon dioxide involved into hydrates during the replacement phase are higher than methane entrapped during the first step. Comparing these two values, the difference clearly appears: before replacement, formed methane hydrates are in the range 0.059–0.103 mol, while carbon dioxide hydrates formed during replacement are in the range 0.085–0.206 mol. Several factors caused that difference. Reactor free volume for hydrate formation in particular contained 235 cm^3 before CH_4 hydrate formation and less for CO_2 formation, due to the presence of already formed solid structures; thus, the lower presence of already existing hydrates led to a greater space and free water availability for new hydrate formation. Also, methane hydrate dissociation was particularly pronounced, with a consequent higher replacement rate.

The final amount of CO_2 hydrates is given by the sum of two different contributions: new structure formation and replacement of methane in already existing water cages. As explained previously, the first quantity increased, but it is not directly related to the replacement process, so it cannot be taken into account for considerations about replacement process efficiency. On the contrary, the consistent methane hydrate dissociation was directly related to a more effective replacement, which led to an efficiency improvement. Moles

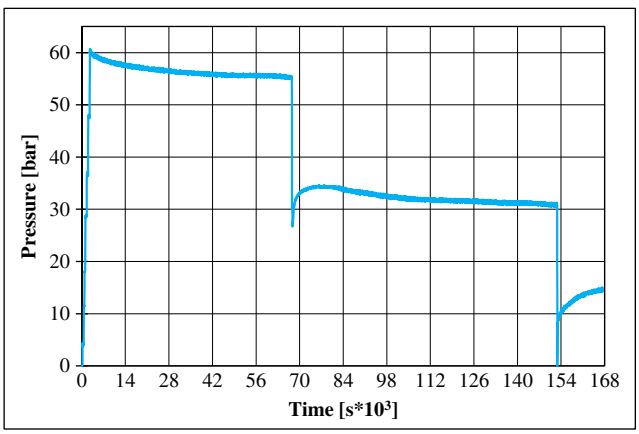

Fig. 11 Pressure over time in test C

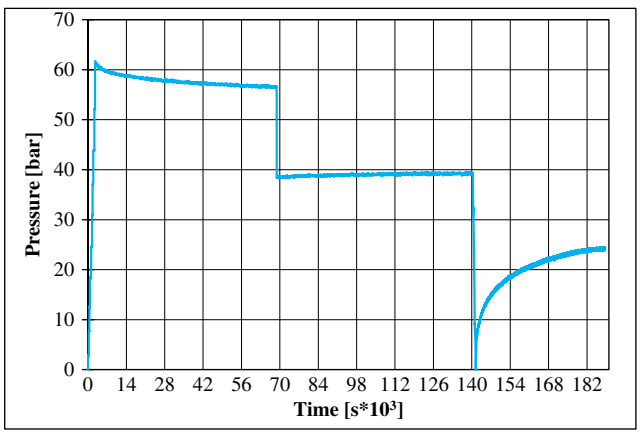

Fig. 13 Pressure over time in test D

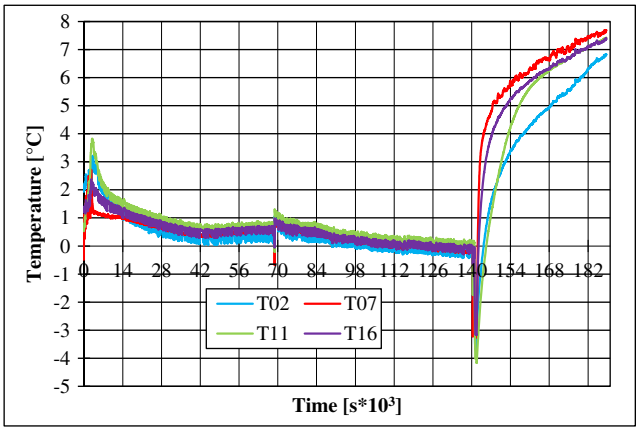

Fig. 14 Temperature over time in test D

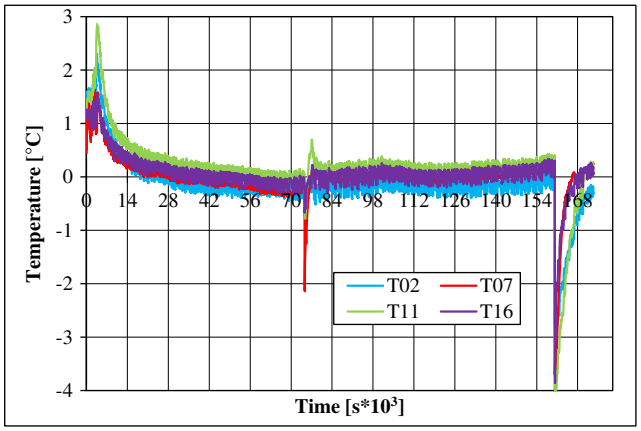

Fig. 16 Temperature over time in test E

of methane remained into water cages are in the range 0.023–0.042, or a little part of the initial quantity, lower of the respective value measured in tests without salt and available elsewhere in literature.

Thus, sodium chloride presence improves the replacement process efficiency and is able to increase the percentage of carbon dioxide storage. Nevertheless, a precise definition of replacement process efficiency needs of a clear distinction between these two quantities.

In Figs. 7, 8, 9, 10, 11, 12, 13, 14, 15 and 16, pressure and temperature trend over time for all tests done is provided.

About temperature diagrams, the first peak indicates that hydrate formation reaction began; the reaction exothermic behaviour is particularly pronounced during first nucleus constitution and, in contained volumes as the used experimental apparatus, causes a sudden temperature increase. In all tests, immediately after that peak occurred, pressure began to decrease and continued until reaching stability, then it remained constant. Temperature variation in the middle of each respective diagram is simply due to the reactor opening for carbon dioxide injection and methane ejection; it has no scientific relevance. However, it may be useful for graphically dividing the two phases which compose all tests and also to understand

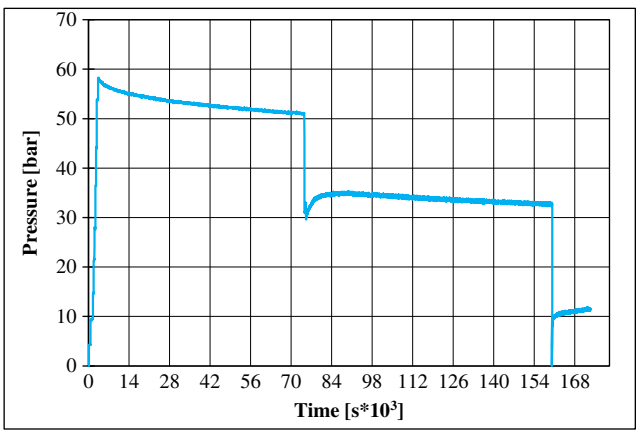

Fig. 15 Pressure over time in test E

if CO_2 hydrate reaction started during its injection or immediately after. Diagrams' part at left of that temperature peak describe CH_4 hydrate formation, as Figs. 4 and 5, while the right side of each figure is related to the replacement process. In this case, plots describing pressure–temperature curves are not useful because the process involves both species and thermodynamic conditions do not permit methane hydrate equilibrium, making that kind of diagram not useful for further considerations. In the same way, in pressure diagrams, the two phases are divided by the pressure decrease present in the middle (it obviously occurred in correspondence of the temperature peak), which was generated for promoting the replacement phase. About that temperature peak, even if the procedure adopted is similar in all test, in some cases, thermocouples registered a decrease in temperature, while in other cases, the contrary occurred. Temperature decrease is due to gas expansion inside the reactor which accompanied pressure reduction, while its increase proves hydrate formation during the injection phase, due to heat released by the reaction. The final temperature drop is related to the complete ejection of gaseous compound from the inlet, in order to allow and properly evaluate hydrate dissociation. In pressure diagrams, the difference between trend CH_4 hydrate formation and CO_2 replacement phase needs to be deepened. In all tests, during the first phase, only methane hydrate formation occurred, with the consequent pressure decrease clearly visible in all diagrams. On the contrary, the replacement phase described the balancing between CH_4 hydrate dissociation, which provoked an increase in pressure and CO_2 hydrate formation and the respective pressure reduction. That explains why the massive CO_2 hydrate formation was not accompanied by pressure decrease. Pressure trend in Figs. 11 and 15 well described that aspect. Immediately after pressure decrease carried out for promoting CO_2/CH_4 replacement, an initial increment was registered, proving how in that phase the leading parameter is methane hydrate dissociation; then, pressure slightly decreased due to the prevalence of CO_2 hydrate formation. In this sense, pressure decrease is more related to new structure

formation than CO_2 hydrates originated by the replacement process.

Conclusions

The present work makes part of a wider experimental research involved in defining how sodium chloride intervenes in the CO_2/CH_4 exchange process into natural gas hydrate reservoirs and what about possibilities of exploiting its characteristic for improving the process efficiency.

Firstly, hydrate formation in presence of 37 g/l of sodium chloride was performed for both species. Results proved the inhibitor potential which salt assumed during the process, suggesting the possibility of a selective behaviour in function of the guest specie present into water cages. Topic of this paper is verifying if a chemical inhibitor (salt in this case) may be considered helpful during the CO_2 replacement application. The last part of experimental section describes five tests in which CO_2/CH_4 exchange was carried out via depressurization. As expected, salt brought to a lower methane hydrate formation during the first phase of all test (which was in the range 0.059–0.103 mol). A particularly positive response came from the total amount of carbon dioxide involved in hydrate formation (0.085–0.206 mol), which had a dual provenience: a higher new structure formation, favoured by a higher space and free water available for the process, due to a previous lower CH_4 hydrate formation and a greater CO_2/CH_4 replacement rate. Methane contained into hydrates after the formation process was particularly contained (in the range of 0.023–0.042 mol), proving that the greatest part of hydrates, composing the lab-scale reservoir, were interested in the replacement process. Finally, experimental results reached in this work brought to the following conclusion: even if sodium chloride is a chemical inhibitor for hydrate, it may be considered a potential allied for improving the CO_2/CH_4 exchange process into natural gas hydrate reservoirs. In particular, it may be helpful for both increasing the quantity of methane recovered and also the quantity of carbon dioxide permanently stored in solid form. Thus, the suggestion of considering another coupling between strategies used for intervening in hydrate reservoirs, rather than the combination of depressurization and thermal stimulation, or the adoption of chemical inhibitors, such as sodium chloride, together with CO_2 replacement strategies. In this experience, NaCl was selected for its diffused presence in correspondence of seafloor reservoirs, its low cost and the neutral impact on hydrate environment. In further works, the adoption of other typologies of chemical inhibitors will be investigated.

Funding Open access funding provided by Università degli Studi di Perugia within the CRUI-CARE Agreement.

References

Aregba AG (2017) Gas hydrate—properties, formation and benefits. Open J Yangtze Gas Oil 2:27–44. https://doi.org/10.4236/ojogas.2017.21003

Babu P, Linga P, Kumar R, Englezos P (2015) A review of the hydrate based gas separation (HBGS) process for carbon dioxide precombustion capture. Energy 85:261–279

Boswell R, Collett TS (2011) Current perspectives on gas hydrate resources. Energy Environ Sci 4:1206–1215

Gambelli AM (2018) Natural gas recovery from hydrate compounds using CO2 replacement strategies: experimental study on thermal stimulation. Energy Procedia 148:647–654

Gambelli AM, Rossi F (2019) Natural gas hydrate: comparison between two different application of thermal stimulation for performing CO2 replacement. Energy 172:423–434

Gambelli AM, Castellani B, Nicolini A, Rossi F (2019a) Gas hydrate formation as a strategy for CH4/CO2 separation: experimental study on gaseous mixtures produced via Sabatier reaction. J Nat Gas Sci Eng 71:102985

Gambelli AM, Filipponi M, Nicolini A, Rossi F (2019b) International Multidisciplinary GeoConference: SGEM; Sofia Vol. 19, Fasc. 4.1 : 333 – 343. Sofia: Surveying Geology & Mining Ecology Managment (SGEM). https://doi.org/10.5593/sgem2019/4.1/S17.043

Gambelli AM, Castellani B, Nicolini A, Rossi F (2019c) Experimental study on natural gas hydrate exploitation: optimization of methane recovery, carbon dioxide storage and deposit structure preservation. J Pet Sci Eng 177:594–601

Ginsburg GD, Soloviev VA (1998) Submarine gas hydrates. VNII Okeangeologia, Saint Petersburg, p 321

Lee Y, Choi W, Seo YJ, Lee JY, Lee J, Seo Y (2018) Structural transition induced by cage dependent guest exchange in CH4 + C3H8 hydrates with CO2 injection for energy recovery and CO2 sequestration. Appl Energy 228:229–239

Li B, Liang YP, Li XS, Wu HJ (2015) Numerical analysis of methane hydrate decomposition experiments by depressurization around freezing point in porous media. Fuel 159:925–934

Liang YP, Liu S, Zhao WT, Li B, Wan QC, Li G (2018) Effects of vertical center well and side well on hydrate exploitation by depressurization and combination method with wellbore heating. J Nat Gas Sci Eng 55:154–164

Linga P, Kumar R, Englezos P (2007) The clathrate hydrate process for post and precombustion capture of carbon dioxide. J Hazard Mater 149(3):625–629

Mel'nikov NN, Kalashnik AI (2011) Geodynamic aspects of the development of offshore oil and gas deposits: case study of Barents region. Water Res 38(7):896–905

Mori YH (2003) Recent advances in hydrate-based technologies for natural gas storage—a review. J Ind Chem Eng (China) 54(1)

Moridis G, Reagan M, Kim SJ, Seol Y, Zhang K (2009) Evaluation of the gas production potential of marine hydrate deposits in the Ulleung Basin of the Korean East Sea. SPE J 14:759–781

Myshakin EM, Ajayi T, Anderson BJ, Seol Y, Boswell R (2016) Numerical simulations of depressurization-induced gas production from gas hydrates using 3-D heterogeneous models of L-Pad, Prudhoe Bay Unit, North Slope Alaska. J Nat Gas Sci Eng 35: 1336–1352

Paull CK, Dillon WP (2001) In: Dillon (ed) Natural gas hydrates; occurrence, distribution and detection. American Geophysical Union, Washington, DC

Rossi F, Gambelli AM, Sharma DK, Castellani B, Nicolini A, Castaldi MJ (2019) Simulation of methane hydrates formation in seabed deposit and gas recovery adopting carbon dioxide replacement strategies. Appl Therm Eng 148:371–381

Shagapov VS, Khasanov MK, Musakaev NG, Duong NH (2017) Theoretical research of the gas hydrate deposits development using the injection of carbon dioxide. Int J Heat Mass Transf 107:347–357

Shin K, Kumar R, Udachin KA, Alavi S, Ripmeester JA (2012) Ammonia clathrate hydrates as new solid phases for Titan, Encedadus, and other planetary systems. Proc Natl Acad Sci U S A 109:14785–14790

Sloan ED Jr (2003) Fundamental principles and applications of natural gas hydrates. Nature 426(6964):353–359

Sloan ED, Koh CA (2008) Clathrate hydrates of natural gases, 3rd edn. CRC Press, Taylor & Francis Group, New York

Sultan N, Choconat P, Canals M, Cattaneo A, Dennielou B, Haflidason H et al (2004a) Triggering mechanism of slope instability processes and sediment failures on continental margins: a geotechnical approach. Mar Geol 213(1-4):291–321

Sultan N, Choconat P, Foucher JP, Mienert J (2004b) Effect of gas hydrate melting on seafloor slope instability. Mar Geol 213(1-4):379–401

Sun F, Yao Y, Li G, Li X (2018a) Geothermal energy development by circulating CO2 in a U-shaped closed loop geothermal system. Energy Convers Manag 174:971–982

Sun F, Yao Y, Li G, Li X, Li Q, Yang J, Wu J (2018b) A coupled model for CO2& superheated steam flow in full-length concentric dual-tube horizontal wells to predict the thermophysical properties of CO2 & superheated steam mixture considering condensation. J Pet Sci Eng 170:151–165

Sun F, Yao Y, Li G, Li X (2018c) Performance of geothermal energy extraction in a horizontal well by using CO2 as working fluid. Energy Convers Manag 171:1529–1539

Takeyaa S, Kida M, Minami H, Sakagami H, Machikubo A, Takahashi N, Shoji H, Soloviev V, Wallmann K, Biebow N, Obzhirov A, Salomatin A, Poort J (2006) Structure and thermal expansion of natural gas clathrate hydrates. Chem Eng Sci 61:2670–2674

Xu C-G, Li X-S (2014) Research progress of hydrate-based CO2 separation and capture from gas mixtures. RSC Adv 35:18301–18316

Yu D, Zhao J, Sun S (2018) Dissociation enthalpy of methane hydrate in salt solution. Fluid Phase Equilib 456:92–97